VOL. 7, NO. 1, JANUARY 2012 ISSN 1819-6608
ARPN Journal of Engineering and Applied Sciences


www.arpnjournals.com

HEAT TRANSFER ANALYSIS IN PCM FILLED RCC ROOF FOR THERMAL MANAGEMENT

M. Ravikumar[1] and P. S. Srinivasan[2]
[1]Department of Mechanical Engineering, Bannariamman Institute of Technology, Sathyamangalam, India
[2]Department of Mechanical Engineering, Knowledge Institute of Technology, Salem, India
E-mail: kumarmravi74@yahoo.co.in

ABSTRACT

Analysis of heat transmission across three roof structures viz., bare RCC roof, RCC roof with weathering coarse and RCC roof with PCM (Phase Change Material) above RCC, are analyzed. A transient numerical procedure is developed. The numerical procedure is validated against the available experimental data. The simulation is carried out on 365 days of year for these three roofs. The PCM melts from 8h to 18h and solidifies during rest of the day. From March to August, the net heat entering into the room per day is positive, thus more and more PCM melts and becomes liquid. The liquid portion of PCM increases from March to August. During September to February, there is a net heat rejection per day, thus the melted PCM becomes solid progressively, and at the end of February, almost all PCM has become solid. Thus there is melting cycle on daily basis and over the year. It takes care of all the external climatic variations and keeps the roof bottom surface temperature almost constant and closes to room air temperature. On yearly basis, about 56% reduction in heat transmission into the room is obtained with PCM roof when compared to the conventional weathering coarse laid roof.

Keywords: heat transfer, building roof, reinforced cement concrete, phase change material, weathering coarse, thermal management.

INTRODUCTION

Phase Change Materials (PCMs) can be used in building walls, ceilings and floors. In building applications, only PCMs that have a phase transition close to human comfort temperature (20-28ºC) can be used. Some Commercial PCMs have also been developed for building applications.

The method of PCM incorporation into building products was analyzed by Hawes and Feldman [1]. The PCM incorporation method comprises of immersion, encapsulation and direct incorporation. Latent heat storage (LHS) system was designed and tested by Arkar and Medved [2] to provide the ventilation for a building. Stritih and Novak [3] designed a solar wall containing black paraffin wax for building ventilation, which absorbs about 79% of solar energy falling on it and energy stored was utilized for heating and ventilating the house.

A finite difference method based thermal building simulation program was designed by Stetiu and Feustel [4] to evaluate the latent heat storage performance of PCM treated wallboard. The peak power demand can be reduced by utilizing thermal mass for downsizing the cooling or heating requirements.

The parameters influencing the energy absorption of the PCM impregnated wall board was tested by Neeper [5] and concluded that it was by melting temperature of PCM, melting range and latent heat capacity of PCM. An experimental and numerical simulation study was conducted by Athienitis *et al*., [6] with PCM gypsum board as inside wall lining and found that the PCM wallboard reduces the room temperature by 4 °C during the day time and reduces the heating load at night drastically.

Lee *et al*., [7] have conducted the thermal performance test with concrete block and PCMs (BS and commercial paraffin) impregnated concrete block and results shown that concrete blocks are able to store the latent and sensible heats of the incorporated PCM, and also the sensible heat of concrete. Hadjieva *et al*., [8] used sodium thiosulphate pentahydrate (Na2S2O3.5H2O) as a PCM for concrete impregnation and they achieved 60% incorporation by adding in the pores and capillary spaces of the concrete.

The investigation of combining PCM with wood-lightweight concrete was done by Mehling *et al*., [9]. The results show that the variation of mechanical properties was not significant. It leads to the usage of shape stabilised PCM for under floor electric heating system which avoids the PCM leakage problem.

This system gets charged by using low cost night time electricity and discharges the stored heat during day time. Zhang *et al*., [10] used the concrete mixed with shape-stabilized PCM material for the building component. They found that the melting temperature of shape-stabilized PCM can be adjusted by using different paraffin and for the electric under-floor space heating system; the optimal melting temperature is about 40°C. Cabeza *et al*., [11] conducted a test in encapsulation of PCM in the concrete walls and the study reveals that the energy storage in the walls leading to an improved thermal inertia, compared with the conventional concrete without phase change materials which has shown the opportunity in energy savings for buildings.

Griffiths *et al*., [12] tested micro encapsulated PCM slurry in a test chamber, containing a chilled ceiling with a phase change temperature around 18°C and the results show that a concentration of 40% microcapsules containing PCM can be used as the heat transfer fluid in the ceiling and also as energy storage medium. It will absorb energy at a set point and avoids increase in panel surface temperature. It also requires a low fluid flow rate, which reduces pumping power requirements.

A double layer PCM concept used for the thermal management in a residential building was studied by Velraj *et al*., [13]. In the present investigation, a year round performance of PCM filled RCC roof is analysed with a view to understand the heat transmission and energy saving aspects when compared to the conventional RCC with weathering coarse laid roof.

MATERIALS AND METHODS

Heat transmission across three roof structures (named as RCC, WC and PCM) shown in Figure-1 are investigated.

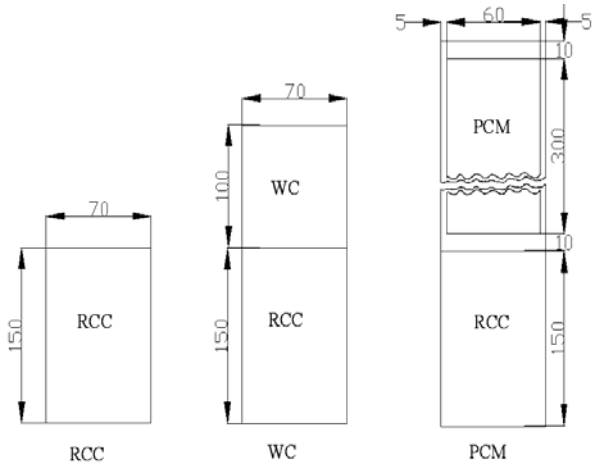

Figure-1. Roof structures.

The roof named RCC is a bare RCC roof of 150 mm thickness and WC has RCC roof of 150 mm thickness and a weathering coarse (made of lime and brick marter) of 250 mm thickness. The PCM roof has a hollow brick tile laid over RCC. The RCC portion has 150 mm thickness. The hollow clay tile (HCT) has 70 mm x 320 mm outer dimensions, which has a rectangular passage of 60 mm x 300 mm. The dimension of the hollow portion is arrived by trial and error to hold about 14 kg of PCM which is needed to take care of summer-winter cycle during the year. The hollow passage is filled with PCM and the ends are closed. The related dimensions also are shown Figure-1.

Figure-1 shows a portion of repetitive symmetry of the roof of room. The same section is repeated for the entire width of the room or build up area. Similarly the hollow passage extends to the entire length of the room. So the problem reduces to a two dimensional transient heat conduction problem. In case of PCM roof, melting and solidification of PCM will also present in the PCM region. The analysis of heat transfer across the roof structure becomes solving a two dimensional transient heat conduction equation, with phase change in its PCM region.

For the mathematical formulation of the problem, the following assumptions are involved.

i) Two dimensional heat conduction in the composite wall.
ii) The thermal properties (thermal conductivity, specific heat, density, latent heat values) are constant and do not vary with temperature.
iii) The PCM is homogeneous and isotropic and convection effects in the molten PCM are negligible.
iv) The internal thermal resistances are negligible.
v) For modelling purpose, the melting or solidification is assumed to take place over a small temperature range ΔTm = (Tm2-Tm1). Thus the specific heat of PCM will vary as follows.

$T < Tm1$, $Cp = Cps$
$T > Tm2$, $Cp = Cpl$
$Tm1 < T < Tm2$, $Cp = LH/\Delta Tm$;
$\Delta Tm = Tm2 - Tm1$

Where Tm1 and Tm2 are the beginning and ending temperature of melting and LH is the latent heat of fusion or melting.

$$k_i \frac{\partial^2 T_i}{\partial x^2} + k_i \frac{\partial^2 T_i}{\partial y^2} = \rho_i C_{pi} \frac{\partial T_i}{\partial \tau}, \quad i = 1,2,3 \tag{1}$$

Where i = 1 for RCC, i = 2 for weathering coarse or HCT and i = 3 for PCM. The same equation holds good for all the three material regions by incorporating suitable k, ρ, Cp values. On the roof top portion (x = 0), solar radiation absorption, convection heat transfer to the atmospheric air and re-radiation to the sky simultaneously exists.

$$k_i \left.\frac{\partial T}{\partial x}\right|_{x=0} = \alpha I_{sol} + \sigma\varepsilon(T^4 - T_{sky}{}^4) + h_o (T - T_{atm}) \tag{2}$$

Where α is the absorptivity of roof, Isol is the solar radiation intensity falling on the roof surface, ε is the emissivity of the roof, Tsky is the sky temperature assumed as Tatm-12 [14] and Tatm is the surrounding atmospheric air temperature. α = 0.4 and ε = 0.4 are used and for calculating ho, the procedure discussed in [14] is used. The solar radiation and atmospheric data are measured over the year (location, Sathyamangalam, Tamilnadu state, India 77°15'E, 11°31'N) are used. On the roof bottom surface, an air-conditioned room at (Troom = 25°C) is assumed.

ANSYS-Fluent 12 finite volume method based software is used for solving the problem. Time step of 60 seconds is used. Before solving the present problem, based on the procedure established here, a case [13] for which experimental results are available is solved to validate the procedure. The heat flux entering into the room over a day has been taken to compare the present procedure and the experimental results. It is observed that the difference is less than 4.2% for the two months data. Thus, the present numerical procedure is suitable for analysing the present problem under investigation. The radiation heat exchange inside the room is considered negligible.

$$k_i \left.\frac{\partial^2 T}{\partial x^2}\right|_{x=xm} = h_i (T - T_{room}) \tag{3}$$

hi is the heat transfer coefficient between the room air and roof bottom, hi = 6.13 [Wm-2K] is used [14]. Due to

repetitive symmetry, left and right side surface of the computational domain are treated as adiabatic i.e.

$$k_i \left.\frac{\partial T}{\partial y}\right|_{y=0} = 0; \quad k_i \left.\frac{\partial T}{\partial y}\right|_{y=ym} = 0 \tag{4}$$

The material properties used in the analysis are given in Table-1. For solving the problem, ANSYS-Fluent 12 finite volume method based software is used. Time step of 60 seconds is used. Grid dependence of the results is verified and grid-independent results are presented. Before solving the present problem, based on the procedure established here, a case [13] for which experimental results are available, is solved to validate the procedure. The heat flux entering into the room over a day has been taken to compare the present procedure and the experimental results.

It is observed that the difference is less than 4.2% for the two months data. Thus, the present numerical procedure is suitable for analyzing the present problem under investigation.

Table-1. Material properties.

Material		**Density, P** (kg/m^3)	**Thermal conductivity, k** (W/mK)	**Specific heat, Cp** (J/kgK)
RCC		2300	1.279	1130
Weathering coarse (WC)		1300	0.25	800
HCT		1300	0.25	800
PCM	Solid	814	0.35	1900
	Liquid	775	0.149	2200
	Melting temp (°C)	28.2	Latent heat (J/kg)	245000

The composite wall taken for analysis is initially maintained at 25°C to start the solution. The problem is solved for 3 days and the temperature distribution at the mid night of the third day is assumed as the initial condition. Then the problem is solved for 31days with March month data as the boundary condition.

The temperature distribution at the end of the previous month last day midnight is used to carry out the solution for the next month. Likewise, the solution procedure is executed till the end of February month, i.e., for 365 days. The results obtained so are presented and discussed in the next section.

RESULTS AND DISCUSSIONS

The atmospheric temperature and the solar radiation data applied during July are shown in Figure-2.

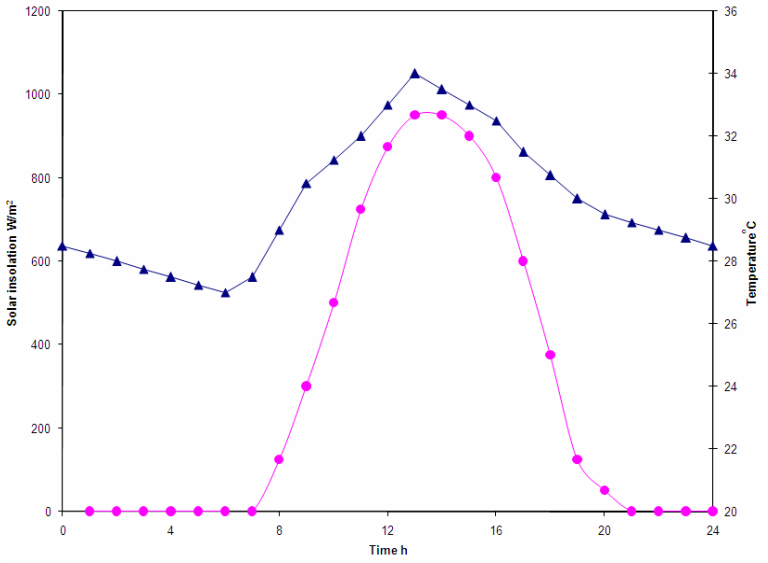

Figure- 2. Variation of atmospheric temperature and solar radiation on the roof surface over 24 hours of the day on 15th July.

Temperature distribution across the roof structure

The variation of temperature across the roof structure during the summer month, 15th July is shown in Figures 3(a), 3(b) and 3(c). The top surface of the roof is taken as x = 0 and the bottom surface is taken as x_m and the distance is normalized as $X^* = x/x_m$.

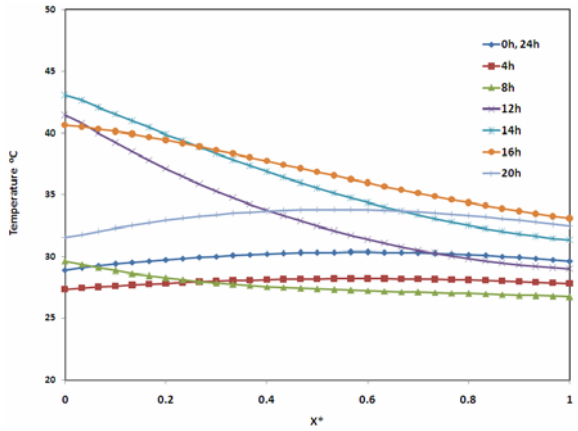

Figure-3(a). Temperature distribution across the RCC roof structure on 15th July.

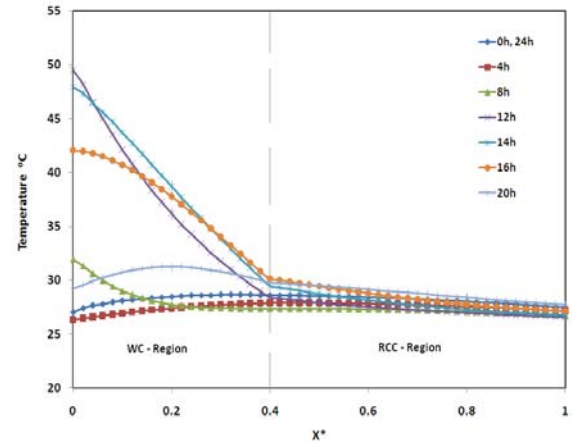

Figure-3(b). Temperature distribution across the WC roof structure on 15th July.

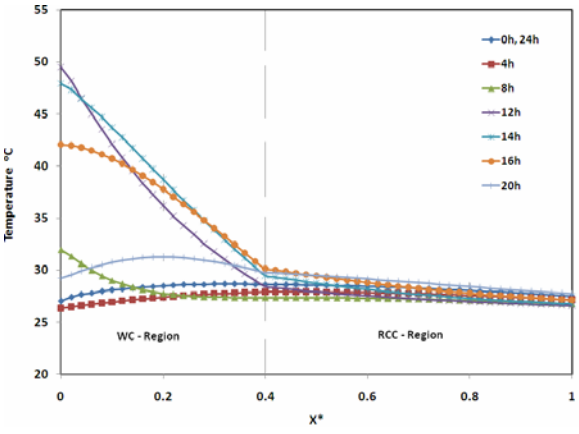

Figure-3(c). Temperature distribution across the PCM roof structure on 15th July.

Due to low thermal inertia, RCC roof shows faster response to the variation in the external weather conditions. During 20h to 8h, heat is lost from the roof to the external atmosphere. Thus the roof temperature drops continuously. Due to increase in atmospheric air temperature and incident solar radiation, the roof temperature continuously raises during 8h to 14h. From the 14h to 20h the temperature of roof near top decreases, however that in the bottom portion of the roof raises as the heat stored at the middle moves on the both the directions. In general, the roof top surface temperature varies from 27ºC to 43ºC, and that at the roof bottom varies in the range 26.5ºC - 34ºC over the day during July.

In case of WC roof, due to more thermal resistance offered by the weathering coarse portion, the variation in external climate is damped in the WC portion and lesser fluctuations are observed in the RCC portion of the roof. The roof top surface varies in the range 26ºC to 49ºC and the bottom surface temperature varies in the range 26ºC to 28ºC. In case of PCM laid roof, all the external variations are observed by melting and solidification of PCM and least fluctuation is noticed in the RCC portion of roof.

The melting and solidification of PCM over the day is shown in Figure-4. The melt fraction of 1.0 represents fully melted and 0.0 represents 100% solid. At 6h, a thin layer of PCM at the roof top side about 80% of PCM at the bottom side are in solid phase, and in between is in liquid phase. Due to heat entering into the roof top, the thin solid PCM at roof top side starts melting from 8h onwards and it is fully melted around 12h. Melting of PCM at the bottom portion happens from 12h onwards and up to 18h. From 18h onwards, outside temperature are lower than the roof top temperature, thus heat is rejected from the roof to the outside air. Thus, the liquid PCM at the top layer starts solidifying from 18h onwards and proceeds up to 6h in the next day morning. As more heat entered in to the roof than that is rejected, the total area of melted zone has increased.

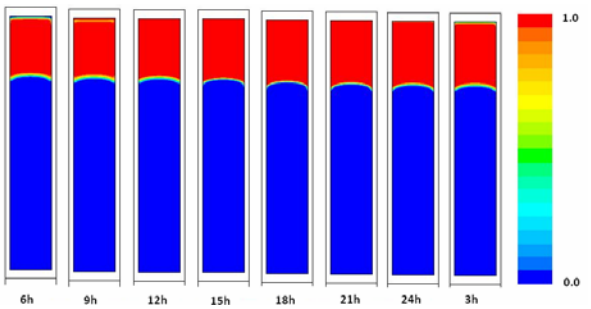

Figure-4. Melt fraction during various hours on 15th of July.

Heat flow into the room across the roof

The melt fraction at 6 AM on the 15th of each month is shown in Figure-5. The area of liquid phase (melt fraction = 1.0) keeps on increasing from March to August). From September to February (winter period), as

more heat is rejected than entering over a day, the area of melted zone is decreasing and becomes very small on 15th February. The process is repeated on each day during all the months. During March to August (summer period), more quantity of heat enters into the roof than that is rejected. Thus there is a net storage of heat in the PCM by melting of more and more PCM region, as shown in Figure-5.

Thus there is one melting and solidification cycle over each day and another cycle over the year. If sufficient volume of PCM is stacked as in this case, a single PCM itself can damp the variations over a day as well as over the year. Because of better damping, the roof bottom temperature remains constant and is close to inside room temperature (25ºC). The roof top surface temperature varies from 27ºC to 49ºC.

The variation of temperature at the RCC portion top (interface-between RCC and WC, and between RCC and HCT in case of WC, and PCM roof structure) and RCC portion bottom over the day on 15th July is shown in Figure-6. The quantity of heat entering in to the room is proportional to the temperature difference between the RCC-portion top and bottom surface temperature.

Lesser the difference, lower is the heat entering into the room, which is preferable. The differences are largest with RCC roof, moderate with WC roof and the least with PCM roof. In case of PCM roof, as all external variations are absorbed by melting and solidification of PCM, the RCC-PCM interface temperature remains constant over the day.

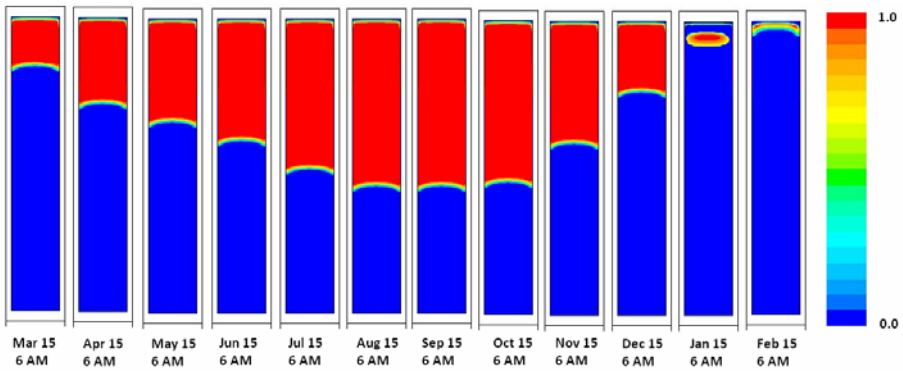

Figure-5. Melt fraction on 15th of each month at 6AM.

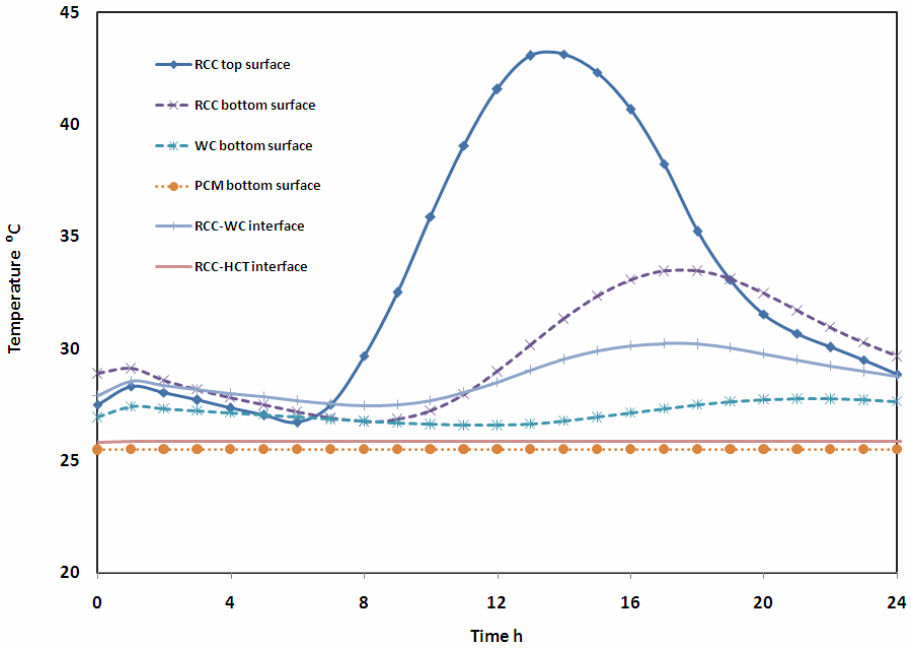

Figure-6. Variation of interface and bottom surface temperature over a day on 15th July.

The total quantity of heat entering into the room over a day through the roof can be calculated by summing up the heat flows through each hour over 24 hours of the day. The heat flow per unit area over a day is calculated for all the 365 days. Such values, averaged over each month, are shown in Table-2.

Table-2. Comparison of thermal performance of roof structures.

Month	Qroom in MJ/m^2-day			% Yearly reduction in PCM roof	
	RCC	WC	PCM	Compared to RCC	Compared to WC
Mar	1.809924	0.806451	0.115938	81.07	55.90
Apr	2.357786	1.010407	0.213743		
May	1.73751	0.736609	0.242375		
June	1.878485	0.782013	0.253436		
July	2.534891	1.136623	0.262332		
Aug	0.918494	0.374009	0.268268		
Sep	1.205171	0.49511	0.271086		
Oct	1.129708	0.466298	0.269773		
Nov	0.508763	0.21715	0.268214		
Dec	0.27224	0.125778	0.265605		
Jan	0.148143	0.039643	0.262226		
Feb	1.078949	0.497819	0.256637		

During February to October, the heat flow into the room with RCC roof is the highest, that with WC roof is moderate and that of PCM roof is the lowest. However, during peak winter, November to January, the heat flow into the room is at par or marginally higher with PCM roof when compared to RCC roof. In fact, it is advantageous to overcome the winter chillness.

On yearly basis, when compared to the bare RCC roof, the heat entering into the room is 57% less with WC roof and 81% less with PCM roof. When compared to the conventional WC roof, the PCM roof offers 56% reduction in heat transmission across the roof, which is significant. In the analysis, an air conditioned room at 25ºC is assumed. Thus about 56% reductions in electricity bill are evident if PCM roof is used instead of the conventional RCC plus weathering coarse roof.

CONCLUSIONS

Heat transfer across three roof structures (RCC, RCC with weathering coarse and RCC with PCM filled) are analyzed numerically over 365 days of the year. The analyses revealed are as follows:

- The thermal inertia of roof is very high, moderate and lowest with PCM, WC and RCC roofs, respectively. Accordingly, the thermal response to external climatic variation is slow, moderate and fast with PCM, WC and RCC roofs, respectively;
- The damping of external climatic variation is moderate with WC roof and very high with PCM roof;
- Incoming heat during daytime is absorbed by melting of PCM and the stored heat is rejected by solidification of PCM during night time. Thus the roof structure below the PCM layer is not affected much by the external climatic variation;
- If sufficient mass of PCM is provided over the RCC portion, there is gradual melting of PCM from March to July (summer season) and the solidification from August to February (winter season). Thus the PCM roof is observed to take care of yearly seasonal variation also;
- Due to better damping provided by PCM, the PCM roof offers the lowest roof bottom surface temperature throughout the year when compared to WC and RCC roofs; and
- On yearly basis about 56% lower heat transmission into the room is observed with PCM roof when compared to WC roof, which has significant and advantageous from energy saving point of view.

REFERENCES

[1] Arkar C., Medved S. 2002. Enhanced solar assisted building ventilation system using sphere encapsulated PCM thermal heat storage. IEA, ECES IA Annex 17, advanced thermal energy storage techniques-feasibility studies and demonstration projects 2nd workshop; Ljubljana, Slovenia.

[2] Athienitis A. K., Liu C., Hawes D., Banu D. and Feldman D. 1997. Investigation of the thermal performance of a passive solar test-room with wall

latent heat storage. Building and Environment. 32: 405-410.

[3] Cabeza. 2007. Use of microencapsulated PCM in concrete walls for energy savings. Energy and Buildings. 39: 113-119.

[4] Feustel H.E. and Stetiu C. 1997. Thermal performance of phase change wallboard for residential cooling application, Lawrence Berkeley National laboratory, Report LBL-38320.

[5] Griffiths P.W. and Eames P.C. 2007. Performance of chilled ceiling panels using phase change material slurries as the heat transport medium. Applied Thermal Engineering. 27: 1756-1760.

[6] Hadjieva M., Stoykov R. and Filipova T. 2000. Composite salt-hydrate concrete system for building energy storage. Renewable Energy. 19: 11-15.

[7] Hawes D.W. and Feldman D. 1992. Absorption of phase change materials in concrete. Solar Energy Material and Solar Cells. 27: 91-101.

[8] Lee T., Hawes D.W., Banu D. and Feldman D. 2000. Control aspects of latent heat storage and recovery in concrete. Solar Energy Material and Solar Cells. 62: 217-237.

[9] Mehling R., Krippner A. and Hauer. 2002. Research project on PCM in wood-light weight concrete. In: Proceedings of the 2nd workshop of IEA ECES IA Annex 17, Ljubljana, Slovenia.

[10] Neeper D. 2000. Thermal dynamics of wall board with latent heat storage. Solar Energy. 68: 393-403.

[11] Pasupathy A. and Velraj R. 2008. Effective of double layer phase change material in building roof for year round thermal management. Energy Building. 40: 193-203.

[12] Stritih U. and Novak P. 2002. Thermal storage of solar energy in the wall for building ventilation. 2nd workshop: IEA, ECESIA Annex 17, advanced thermal energy storage techniques-feasibility studies and demonstration projects, Ljubljana, Slovenia.

[13] Sami A. and Al-Sanea. 2002. Thermal performance of building roof elements. Building and Environment. 37: 665-675.

[14] Zhang Y.P., Lin K.P., Yang R., Di H.F. and Jiang Y. 2006. Preparation, thermal performance and application of shape-stabilized PCM in energy efficient buildings. Energy and Buildings. 38: 1262-1269.